

# Wavefront Deformations in Excitable Media: Chemical Lenses and Ripples

Mario Markus and Kosta Stavridis

*Phil. Trans. R. Soc. Lond. A* 1994 **347**, 601-609

doi: 10.1098/rsta.1994.0069

## Email alerting service

Receive free email alerts when new articles cite this article - sign up in the box at the top right-hand corner of the article or click [here](#)

To subscribe to *Phil. Trans. R. Soc. Lond. A* go to:  
<http://rsta.royalsocietypublishing.org/subscriptions>

# Wavefront deformations in excitable media: chemical lenses and ripples†

BY MARIO MARKUS AND KOSTA STAVRIDIS

*Max-Planck-Institut für molekulare Physiologie, Postfach 10 26 64,  
44026 Dortmund, Germany*

We investigate experimentally the light sensitive Belousov–Zhabotinskii reaction in a silica gel. We focus on two ways of deforming wavefront curvature. In the first one, deformation is imposed by projecting a light spot on the medium rendering refractive phenomena analogous to traditional glass lenses in linear optics. Cellular automata simulations of these ‘chemical lenses’ are in agreement with experiments. The second type of deformation is not imposed on the system but spontaneous; it is due to an instability which is not yet completely understood and which modulates aperiodically the curvature of the wavefronts, causing ‘ripples’.

## 1. Introduction

Manipulation of chemical waves by light and other external means is receiving growing attention. As early as 1973, Busse and Hess reported that a wave can be initialized by ultraviolet irradiation in the ferroin-catalysed Belousov–Zhabotinskii (BZ) reaction. Manipulations using visible light were accomplished by Kuhnert (1983, 1986) and Kuhnert *et al.* (1989). These authors illuminated the reaction catalysed by the ruthenium bipyridyl complex  $\text{Ru}(\text{bpy})_3^{2+}$ . They suggested that this reagent may be used as a highly parallel computational device for image processing. This idea even led to two patents (Agladze *et al.* 1987; Ilyasov *et al.* 1989). Detailed reports on the computational possibilities were given by Holden *et al.* (1991) and by Krinsky *et al.* (1991); these possibilities include: associative memory, distinction between closed and unclosed curves, finding the shortest path in a labyrinth, restoration of broken contours and edge detection. Zülke *et al.* (1989) discussed this system as a learning machine, Yamaguchi *et al.* (1992) as an artificial retina.

In addition to be a potential computational device, the BZ reaction offers a convenient model system for non-uniform reaction-diffusion media. This is interesting because most reaction-diffusion systems in nature, such as biological tissues or ecological systems, have in fact non-uniform control conditions. Work in this context has been performed by Zhabotinskii *et al.* (1993), who used the ferroin-catalysed BZ reaction at spatially varying oxygen concentrations.

In the present work, we investigate the light sensitive BZ reaction catalysed by  $\text{Ru}(\text{bpy})_3^{2+}$ , which permits a faster and easier implementation of non-uniformity

† This paper was produced from the authors’ disk by using the  $\text{\TeX}$  typesetting system.

than the manipulation by oxygen in the system just mentioned. In one of our previous works, we have already used the light sensitive medium to show that a light gradient induces a drift ('phototaxis') of spiral waves (Markus *et al.* 1992).

## 2. Materials and methods

### (a) Experiments

We first prepared a waterglass solution using sodium silicate (from Riedel de Haën), which contains 63%  $\text{SiO}_2$  and 18%  $\text{Na}_2\text{O}$ . 15 g of sodium silicate were dissolved in distilled water (total volume: 100 ml). This was boiled for about 15 min until the solution was clear. After cooling down to room temperature, the solution was filtered.

The  $\text{Ru}(\text{bpy})_3\text{SO}_4$  solution was prepared from  $\text{Ru}(\text{bpy})_3\text{Cl}_2$  as follows. 2.5 g  $\text{Ru}(\text{bpy})_3\text{Cl}_2$  was dissolved in 40 ml  $\text{H}_2\text{O}$  and then made up to 100 ml with 5 M  $\text{H}_2\text{SO}_4$ . After two hours, the precipitate was filtered, dried and made up to 100 ml with 0.025 M  $\text{H}_2\text{SO}_4$ .

Varying concentrations of the Ru-complex between 0.71 mM and 2.8 mM were immobilized in a silica-gel matrix in a petri dish (diameter 6.2 cm, thickness of the gel 0.9 mm). The gel was used to avoid convection, which can destabilize the waves as studied by Markus *et al.* (1987). For the preparation of the gel, see Yamaguchi *et al.* (1991).

The reaction starts after pouring the BZ solution on the top of the gel layer. The volumes of the solution and that of the gel were equal. The initial concentrations in this solution were as follows: 0.18 mM NaBr, 0.33 mM malonic acid, 0.39 mM NaBrO<sub>3</sub> and 0.63 mM  $\text{H}_2\text{SO}_4$ . Due to the diffusive equilibration, these concentrations decreased to a half of their initial value.

All chemicals were of analytical grade and used without further purification. The petri dish was held at  $25 \pm 0.5$  °C. After a few minutes travelling waves appeared spontaneously. As light source we used a slide projector with digital regulation of light intensity (PAXIMAT Multimag 5025 AFI). The parallel beam leaving the projector passed (in normal direction) first an interference filter (450.6 nm, transmission: 56%), then a convergent lens and then (in normal direction) an horizontal diffusion screen, over which the petri dish was placed. The light intensities given here in the figure captions are intensities measured immediately before light enters the reactive solution in the absence of the interference filter. All experiments were done by letting first the waves evolve in the dark for two hours, and then turning light on (a spot for the chemical lenses, and uniform illumination for the ripples). Video images were recorded and digitized.

### (b) Numerical methods

Simulations were performed using a cellular automaton with a semi-random discretization (one point placed randomly within each element of a square grid). This discretization, in connection with a circular neighbourhood  $N$  and local averaging within  $N$ , has proven to yield quantitative agreement with experiments involving excitable media (Markus 1990, 1991; Markus & Hess 1990 *a, b*; Markus *et al.* 1991). Our approach guarantees isotropic propagation, i.e. independence of the wave velocity on spatial orientation. In contrast, other automata approaches (e.g. those by Gerhardt & Schuster (1989), or Gerhardt *et al.* (1990)) do not

always render isotropy. Lacking isotropy, the normal velocity of a wavefront does not depend only on the curvature, as given by the eikonal relationship (Keener & Tyson 1986) but also on the direction of propagation. The latter dependence is a numerical artifact leading to unrealistic distortions in anisotropic automata; formulated in a simple way: waves that should be 'round' often appear as squares with rounded corners.

The states of our automaton are:  $S = 0$  (resting),  $S = 1, 2, \dots, n$  (refractory) and  $S = n + 1$  (excited). We define  $r = R/d$ , where  $R$  is the radius of the circular neighbourhood  $N$  and  $d$  is the side length of the square elements. If  $\nu$  is the number of elements in  $N$  having  $S = n + 1$ , an intermediate state  $\sigma$  is determined by the following rules:

- (1) if  $0 \leq S \leq S_{\max}$  and  $\nu \geq m_0 + pS$ , then  $\sigma = n + 1$ ;
- (2) if  $S = 0$  and  $\nu < m_0$ , then  $\sigma = 0$ ;
- (3)  $\sigma = S - 1$  in any case not yet considered.

The parameters are:  $S_{\max}$ ,  $m_0$ ,  $p$ ,  $r$  and  $n$ . After determining  $\sigma$ , the new  $S$  is calculated by taking the average of  $\sigma$  within  $N$  (unless at the centre of  $N$  is  $\sigma = 0, 1$  or  $n + 1$ , for which we simply set  $S = \sigma$ ). For the determination of the wavefront curvature, both from simulations and from experiments, we used a simple but efficient method. The procedure consisted in setting up a large stock of circles cut out of paper having different radii. We simply held these circles by hand on the graphical output and chose the optimum by trial and error.

### 3. Chemical lenses

We investigate here the possibility of deforming wavefronts, or more precisely: to change their curvatures using refractive effects with light spots. In analogy to the processes occurring in conservative media (Born 1970), we call these light spots 'chemical lenses'.

The concept of refraction of excitable media is not new. In fact, Mornev (1984) studied theoretically the passage of waves from one medium into another one, the media having different diffusion coefficients but identical chemical kinetics. Zhabotinskii *et al.* (1993) showed that Snell's law is obeyed for two media consisting of gels with the ferroin-catalysed BZ reaction, one covered and one uncovered with a glass plate, thus differing in their inhibition by oxygen.

In the present work we used the slide projector to set a circular zone of larger light intensity than in the rest of the petri dish. Figure 1 shows typical behaviours of wave refraction by such a light spot. In particular, figure 1*a, b* shows convex wavefronts entering the lenses and leaving it also as convex waves, but of lower curvature (almost equal to zero in figure 1*b*). In traditional optics, say with a biconvex lens, this is analogous to the situation in which a point object lies within the focal length and leads to a virtual point image on the same side as the object, but farther away from the lens ('magnifying glass'). Figure 1*c* shows a convex wavefront entering the lens and leaving it on the other side as a planar wave. This is analogous to a parallel beam resulting from a point object lying on the focal point on the other side of a traditional lens. Figure 1*d-f* shows convex wavefronts entering the lens and leaving it on the other side as a concave wave (slightly concave figure 1*d* and highly concave in figure 1*e, f*).

Figure 2*a* shows the curvature  $K_{\text{out}}$  of the outgoing wavefront (as it passes the

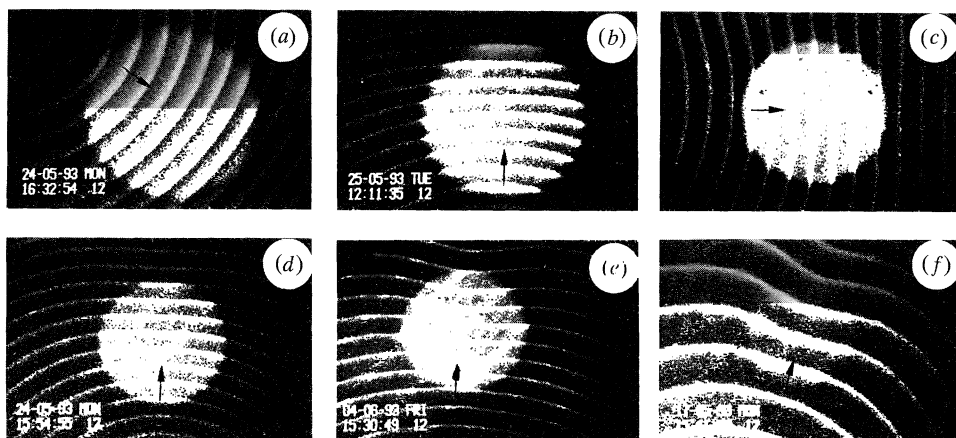


Figure 1. Experiments showing refraction of chemical waves by light spots ('chemical lenses'). The arrows indicate the direction of wave propagation. Spot diameter: 14 mm. Light intensity in the spot: 30 000 lx, outside the spot: 20 000 lx. Ru-concentration: 2.8 mM.

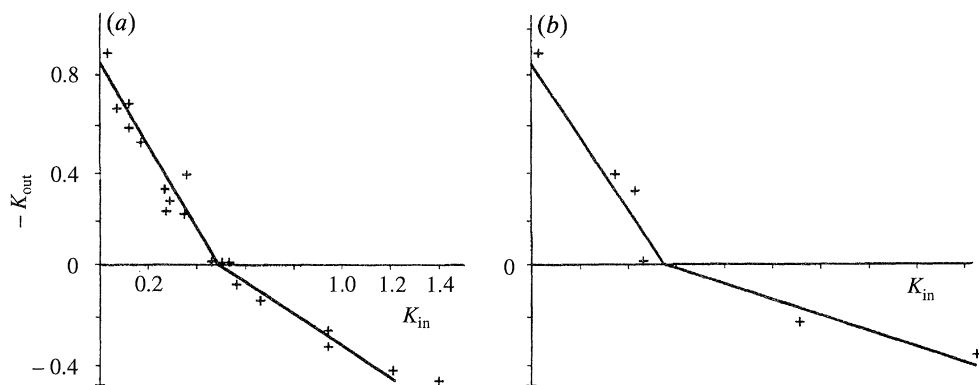


Figure 2. (a) Curvature of the outgoing wavefront ( $K_{\text{out}}$ ) as a function of the curvature of the ingoing wavefront ( $K_{\text{in}}$ ) for the experimental chemical lenses, such as those shown in figure 1 (units:  $\text{cm}^{-1}$ ). (b) The same as on the left, but for simulations, such as those shown in figure 3 (arbitrary units).

border of the spot) as a function of the curvature  $K_{\text{in}}$  of the ingoing wavefront (also as it passes the border of the spot, but on the other side). We define a curvature to have positive (resp. negative) sign if it is convex (resp. concave). Thus, the upper right quadrant of the coordinate system of figure 2a describes ingoing convex waves yielding outgoing concave waves. The lower right quadrant describes both ingoing and outgoing convex waves. In each quadrant, we can approximate the function by a straight line given by

$$\alpha K_{\text{in}} - K_{\text{out}} = 1/f, \quad (3.1)$$

with an effective focal length  $f$ . Note that  $f$  is the distance (from the lens edge) of the centre of curvature of an outgoing wave resulting from ingoing planar waves ( $K_{\text{in}} = 0$ ),  $\alpha f$  is the distance (from the lens edge) of the centre of curvature of an ingoing wave leading to an outgoing planar wave ( $K_{\text{out}} = 0$ ).

In traditional conservative optics with thin lenses, (3.1) is valid with  $\alpha = 1$



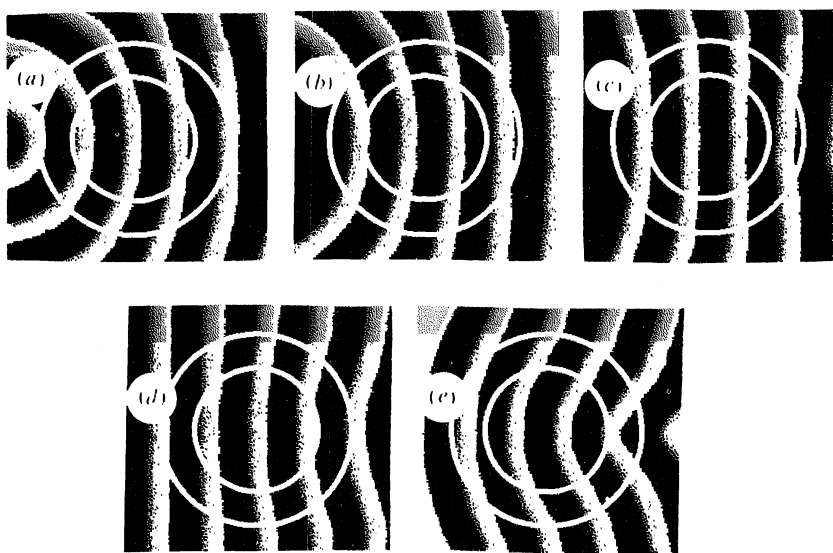


Figure 3. Automaton simulations of chemical lenses. Propagation is from left to right. Inner circle: border of simulated light spot. Outer circle: approximation for the 'limit' of  $\text{Br}^-$  produced in the spot and diffusing outwards. (a)–(c) correspond qualitatively to the experiments shown in figure 1.

if the lens is immersed in a single medium, and with  $\alpha \neq 1$  if the lens is at the interface between different refractive media. The asymmetry  $\alpha \neq 1$  in our case is easy to explain: the eikonal relationship  $V_N = V_N(K)$ , where  $V_N$  is the normal velocity and  $K$  the curvature, is a monotonously decreasing function (see Tyson & Keener 1988); thus convex waves ( $K > 0$ ) are slower than concave ones ( $K < 0$ ) for the same absolute value of  $K$ .

For the automaton simulations of the chemical lenses we used, outside the light spot, the parameters of a previous work (Markus *et al.* 1992):  $r = 5$ ,  $n = 5$ ,  $S_{\max} = 3$ ,  $p = 2$ ,  $m_0 = 5$ . In that work we had assumed that an increase in light intensity corresponds to an increase in the refractory time  $n$ . However, we were not successful with this assumption in the course of the present work: planar waves became discontinuous at the light-dark border but remained planar as they passed through the lens. Instead, we did obtain an approximation of the experimentally observed changes in curvature by assuming that  $m_0$  is larger inside the light spot ( $m_0 = 8$  within a radius of  $45d$ ). Agreement with experiments could be improved by assuming that outside the spot there is a second circle (radius is  $70d$ ) so that  $m_0 = 6$  in the resulting annulus. The two circles are shown in figure 3. The assumption of a transition annulus describes experiments better because of the following reasons. Light in the spot causes an enhanced production of  $\text{Br}^-$  (Kuhnert 1986) and  $\text{Br}^-$  diffuses outwards, where it is degraded; the result is some decreasing  $\text{Br}^-$  concentration profile. Such a profile can certainly be better approximated by a two-step function (two circles) than by a one-step function (one circle). Figure 3a–e shows typical simulations corresponding to experiments (compare with figure 1). Figure 3d,e predicts situations which we have not yet observed experimentally; these situations, which involve planar or concave ingoing waves may be accomplished in future experiments by using the

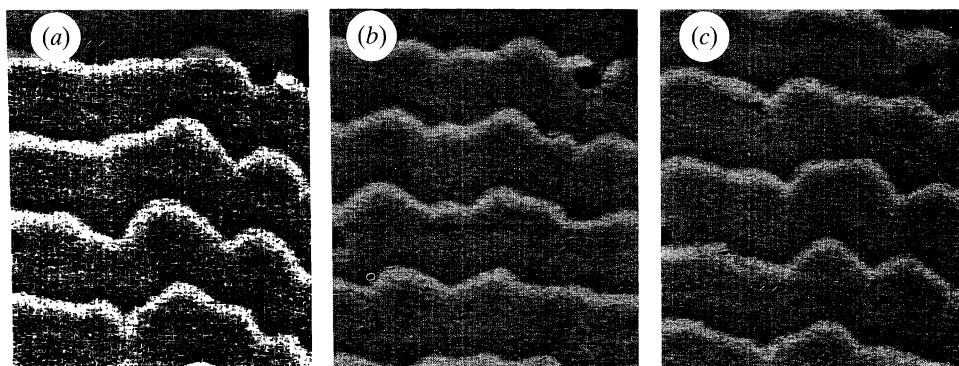


Figure 4. Wavefront instabilities ('ripples') in the same zone of the dish but at different times: (a) 0 min; (b) 3 min; (c) 6 min (30 000 lx, Ru-concentration: 1.0 mM).

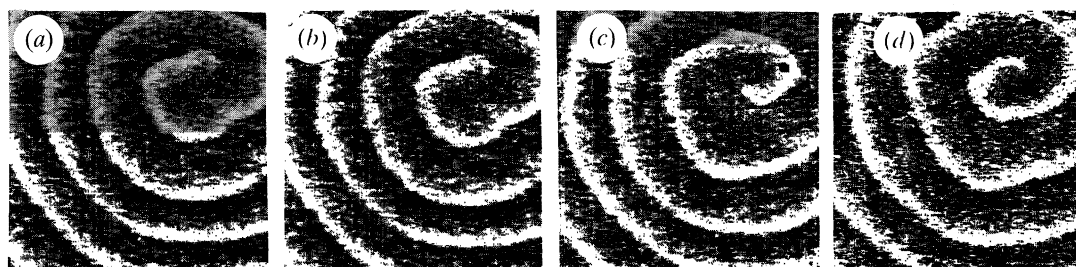


Figure 5. Unstable spiral at the following times: (a) 0 min; (b) 0.68 min; (c) 0.91 min; (d) 1.67 min (10 000 lx, Ru-concentration: 0.71 mM).

outgoing wave of one lens as the ingoing wave of another one. Note that in the particular simulations shown in figure 3 the parameters  $p$  and  $S_{\max}$  play no role because the wavefronts are so isolated from each other that only cells with  $S = 0$  may be excited; thus, we have reduced here the automaton to a three parameter model, while one must keep in mind that in future simulations of waves following close enough to each other one should consider the interaction of wavefronts with the refractory tails ahead of them, as described by  $p$  and  $S_{\max}$ .

The right side of figure 2 shows the relationship between curvatures of ingoing and outgoing waves as it results from the automaton simulations. The curvatures were determined when the wavefront of the ingoing or of the outgoing wave touched the inner circle (see figure 3). Comparison of right side (theoretical) and left side (experimental) of figure 2 reveals satisfactory qualitative agreement concerning a nearly linear relationship in each quadrant, as well as the asymmetry  $\alpha \neq 1$ .

#### 4. Ripples

Instabilities leading to spontaneous wavefront deformations were found in an homogeneously illuminated medium at low Ru-complex concentrations and proper light intensities. These instabilities lead to ripples in the waves, which are aperiodic in space and time.

An example resulting at high light intensity is shown in figure 4. Examples at

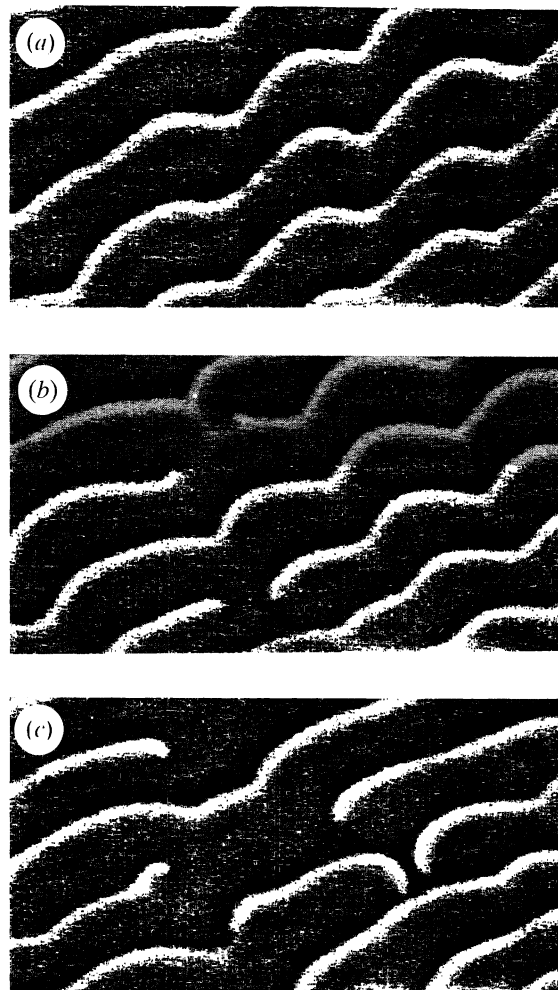


Figure 6. Breakdown of ripples ((a), time 0) into turbulent wave pieces at the following times: (b) 6.88 min; (c) 11.27 min (17 000 lx, Ru-concentration: 0.71 mM).

lower intensities and lower Ru-complex concentrations are given in figures 5 and 6a. Ripples appeared at earliest about 15 min after illumination of waves which have developed in the dark. To make sure that they did not occur due to inhomogeneous light intensity, we displaced the petri dish within the light beam and observed no change. They lasted up to 2 h. However, for certain conditions (e.g. those of figure 6) a few minutes after their appearance, ripples broke down into wave pieces which remained for hours in aperiodic motion. We did not simulate ripples since their mechanism is not yet clear.

## 5. Discussion

We have presented two ways of deforming wavefronts in an excitable medium: a forced deformation using light spots ('lenses') and spontaneous self-deformations due to instabilities ('ripples'). None of these phenomena had been reported before.



The agreement of measurements and simulations of chemical lenses is qualitatively satisfactory. However, it is not clear yet if light influences the refractory time  $n$ , as assumed previously (Markus *et al.* 1992) or the excitation threshold  $m_0$ , as assumed here. We hope this will be clarified in the course of future kinetic investigations following the work of Kuhnert (1986), Krug *et al.* (1990) and Jinguji *et al.* (1992).

Also, the mechanism leading to 'ripples' is unclear. We can exclude instabilities due to the interaction of the reactive solution with the gel, because these instabilities have been shown not to occur at the low waterglass concentration (15%) of the present work (Neumann *et al.* 1993). Also, we are not dealing with the type of instabilities described by Horváth *et al.* (1993), which involve the consumption of a reactant in front of the wave: in our case the relevant reactants are so highly concentrated that fluctuations should not be rate-determining.

Another model for wavefront instabilities has been proposed by Kuramoto (1980, 1984). In that model, lateral inhibition (like in a Turing instability, but travelling with the wave) enhances convexities and concavities. Kuramoto (1980) formulates the condition for instability as  $\nu < 0$ , where  $\nu$  is an effective surface tension. This condition is fulfilled if the effective transport of the activator is slower than that of the inhibitor. In this connection, it should be kept in mind that the effective transport of a substance not only depends on its diffusion coefficient but also on the kinetic constants, in particular being positively correlated to its production rate. Since it is known that light enhances the production of the inhibitor  $\text{Br}^-$  (Kuhnert 1986; Jinguji *et al.* 1992) one may expect that the instability condition can be fulfilled in our case. A determination of  $\nu$  as a function of the kinetic constants and of the diffusion coefficients of the Ru-catalysed BZ reagent is thus desirable to determine the conditions for  $\nu < 0$ . It is also open and desirable to find out if the refractory tails in front of our wavefronts have a destabilizing effect.

We thank Antonio Giaquinta for his idea of introducing two circles in lens simulations, Carsten Schäfer for programming assistance, as well as Stefan Leute and Thomas Düttemeyer for video image processing. Also, we thank Vicente Pérez-Muñuzuri for pointing us to useful literature, as well as Anatol Zhabotinsky, Volodia Zykov and Kenneth Showalter for discussions attempting to explain the ripples. In addition, we thank the Commission of the European Communities (DG XII) and the Engel-Stiftung, Marl, Germany, for financial support.

## References

- Agladze, K. I., Ilyasov, F. E., Krinsky, V. I. & Mornev, O. A. 1987 Patent of the USSR 4280381/24-112818.
- Born, M. 1970 *Principles of optics*. Oxford: Pergamon.
- Gerhardt, M. & Schuster, H. 1989 A cellular automaton describing the formation of spatially ordered structures in chemical systems. *Physica D* **36**, 209–221.
- Gerhardt, M., Schuster, H. & Tyson, J. J. 1990 A cellular automaton model of excitable media involving curvature and dispersion. *Science, Wash.* **247**, 1563–1566.
- Horváth, D., Petrov, V., Scott, S. K. & Showalter, K. 1993 Instabilities in propagating reaction-diffusion fronts. *J. chem. Phys.* **98**, 6332–6343.
- Holden, A. V., Tucker, J. V. & Thompson, B. C. 1991 Can excitable media be considered as computational systems? *Physica D* **49**, 240–246.
- Ilyasov, F. E., Kazanovic, Ya. B. & Krinsky, V. I. 1989 Patent of the USSR 4424588/24-74229.

- Jinguji, M., Ishihara, M. & Nakazawa, T. 1992 Primary process of illumination effect on the  $\text{Ru}(\text{bipy})_3^{2+}$  catalysed Belousov–Zhabotinskii reaction. *J. phys. Chem.* **96**, 4279–4281.
- Keener, J. P. & Tyson, J. J. 1986 Spiral waves in the Belousov–Zhabotinskii reaction. *Physica D* **21**, 307–324.
- Krinsky, V. I., Biktashev, V. N. & Efimov, I. R. 1991 Autowave principles for parallel image processing. *Physica D* **49**, 247–253.
- Krug, H.-J., Pohlmann, L. & Kuhnert, L. 1990 Analysis of the modified oregonator accounting for oxygen sensitivity and photosensitivity of Belousov–Zhabotinskii systems. *J. phys. Chem.* **94**, 4862–4866.
- Kuhnert, L. 1983 Chemische Strukturbildung in festen Gelen auf der Basis der Belousov–Zhabotinsky Reaktion. *Naturwissenschaften* **70**, 464–466.
- Kuhnert, L. 1986 A new optical photochemical memory device in a light-sensitive chemical active medium. *Nature, Lond.* **319**, 393–394.
- Kuhnert, L., Agladze, K. I. & Krinsky, V. I. 1989 Image processing using light-sensitive chemical waves. *Nature, Lond.* **337**, 244–247.
- Kuramoto, Y. 1980 Instability and turbulence of wave fronts in reaction-diffusion systems. *Progr. theor. Phys.* **63**, 1885–1903.
- Kuramoto, Y. 1984 *Chemical oscillations, waves, and turbulence*, ch. 7. Berlin: Springer.
- Markus, M. 1990 Modelling morphogenetic processes in excitable media using novel cellular automata. *Biomed. Biochim. Acta* **bf49**, 681–696.
- Markus, M. 1991 Dynamics of a cellular automaton with randomly distributed elements. In *Mathematical population dynamics* (ed. O. Arino, D. E. Axelrod & M. Kimmel), pp. 413–434. New York: Marcel Dekker.
- Markus, M. & Hess, B. 1990 *a* Isotropic cellular automaton for modelling excitable media. *Nature, Lond.* **347**, 56–58.
- Markus, M. & Hess, B. 1990 *b* Isotropic automata for simulations of excitable media: periodicity, chaos and reorganization. In *Dissipative structures in transport processes and combustion* (ed. D. Meinköhn), pp. 197–214. Berlin and Heidelberg: Springer-Verlag.
- Markus, M., Krafczyk, M. & Hess, B. 1991 Randomized automata for isotropic models of two- and three-dimensional waves and spatiotemporal chaos in excitable media. In *Nonlinear wave processes in excitable media* (ed. A. V. Holden, M. Markus & H.-G. Othmer), pp. 161–182. New York: Plenum Press.
- Markus, M., Müller, S. C., Plessner, Th. & Hess, B. 1987 On the recognition of order and disorder. *Biol. Cybernetics* **57**, 187–195.
- Markus, M., Nagy-Ungvarai, Zs. & Hess, B. 1992 Phototaxis of spiral waves. *Science, Wash.* **257**, 225–227.
- Mornev, O. A. 1984 Elements of the ‘optics’ of autowaves. In *Self-organization. Autowaves and structures far from equilibrium* (ed. V. I. Krinsky), pp. 111–118. Berlin and Heidelberg: Springer-Verlag.
- Neumann, B., Nagy-Ungvarai, Zs. & Müller, S. C. 1993 Interaction between silica gel matrices and the Belousov–Zhabotinskii reaction. *Chem. Phys. Lett.* **211**, 36–40.
- Yamaguchi, T., Kuhnert, L., Nagy-Ungvarai, Zs., Müller, S. C. & Hess, B. 1991 *J. phys. Chem.* **95**, 5831–5840.
- Yamaguchi, T., Ohmori, T. & Matumura-Inoue, T. 1992 Artificial retina. Photoimage processing in the Belousov–Zhabotinskii reaction in gels. In *Spatio-temporal organization in nonequilibrium systems* (ed. S. C. Müller & Th. Plessner), pp. 277–280. Dortmund: Projekt Verlag.
- Zhabotinsky, A. M., Eager, M. D. & Epstein, I. R. 1993 Refraction and reflection of chemical waves. *Phys. Rev. Lett.* **71**, 1526–1529.
- Zülicke, Ch., Ebeling, W. & Schimansky-Geier, L. 1989 Dynamic pattern processing with adaptive excitable media. *Biosystems* **22**, 261–272.



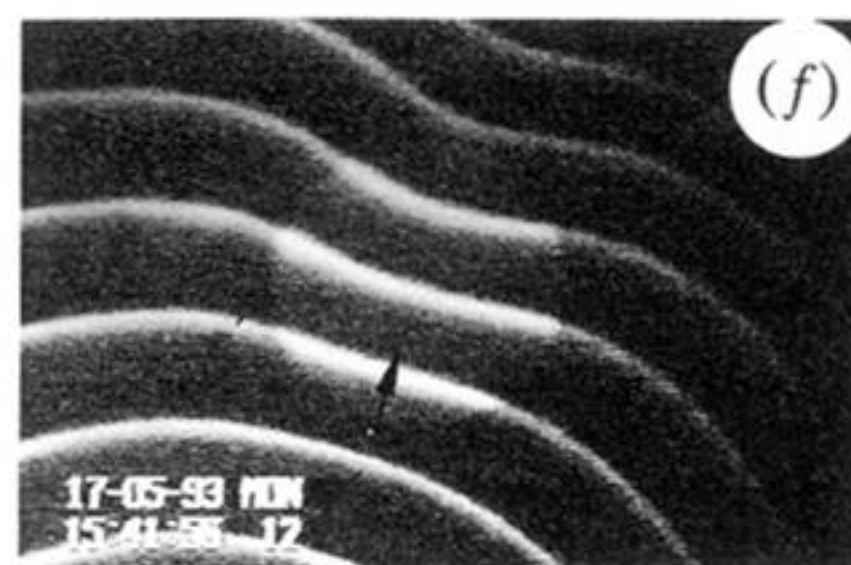
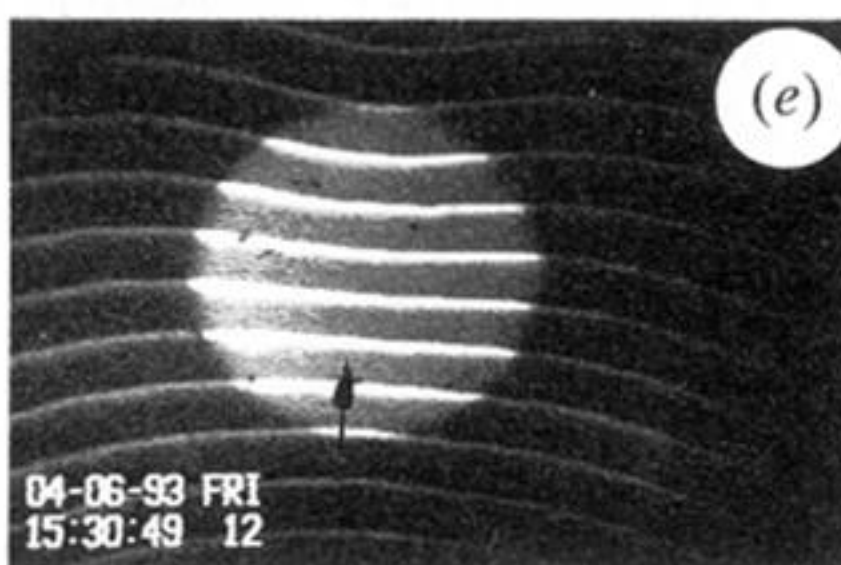
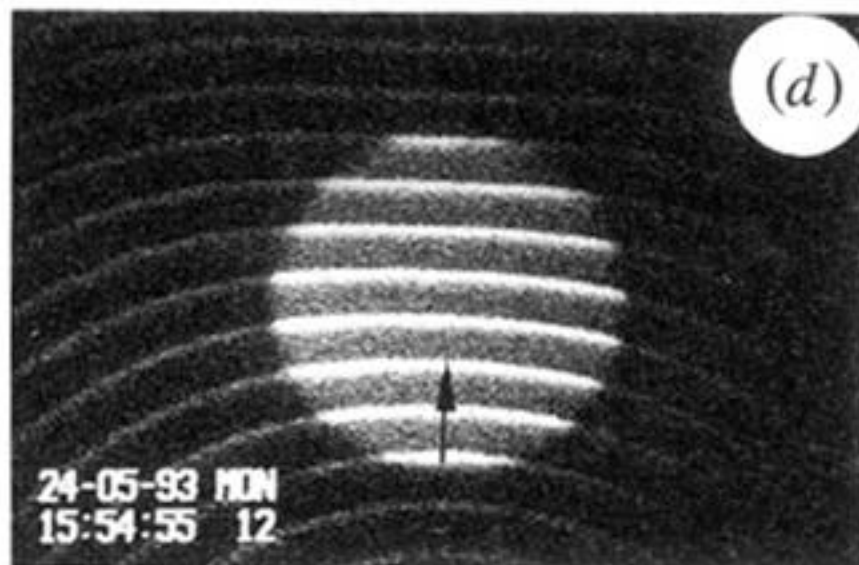
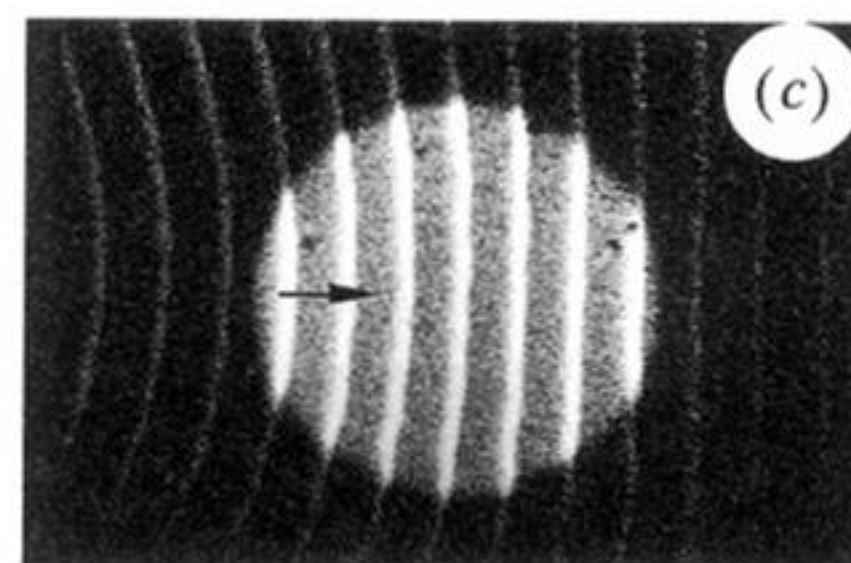
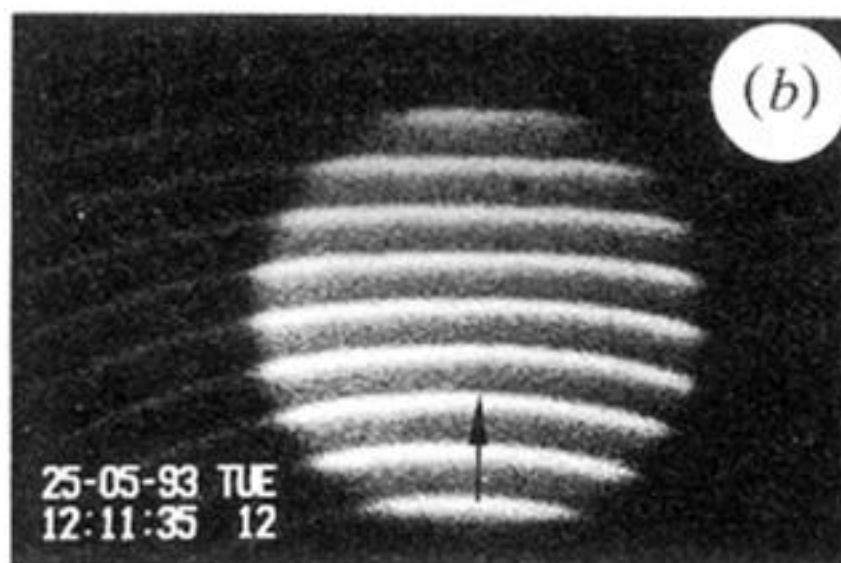
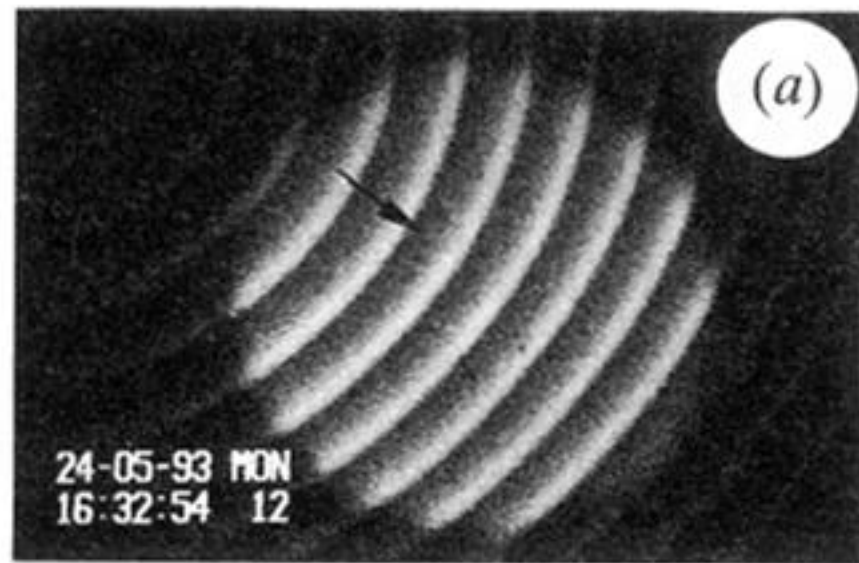


Figure 1. Experiments showing refraction of chemical waves by light spots ('chemical lenses'). The arrows indicate the direction of wave propagation. Spot diameter: 14 mm. Light intensity in the spot: 30 000 lx, outside the spot: 20 000 lx. Ru-concentration: 2.8 mM.



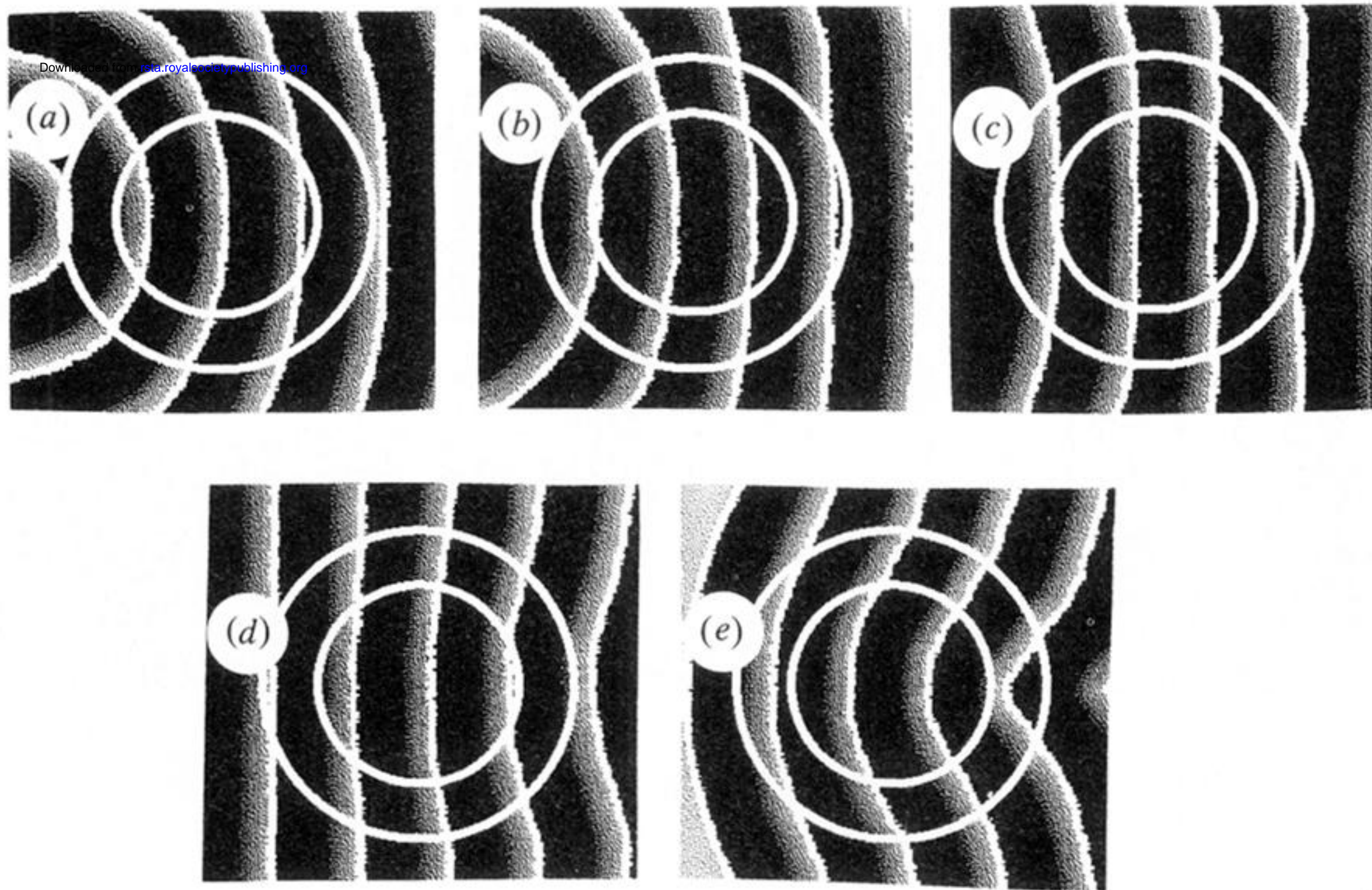


Figure 3. Automaton simulations of chemical lenses. Propagation is from left to right. Inner circle: border of simulated light spot. Outer circle: approximation for the 'limit' of  $\text{Br}^-$  produced by the spot and diffusing outwards. (a)–(c) correspond qualitatively to the experiments shown in figure 1.



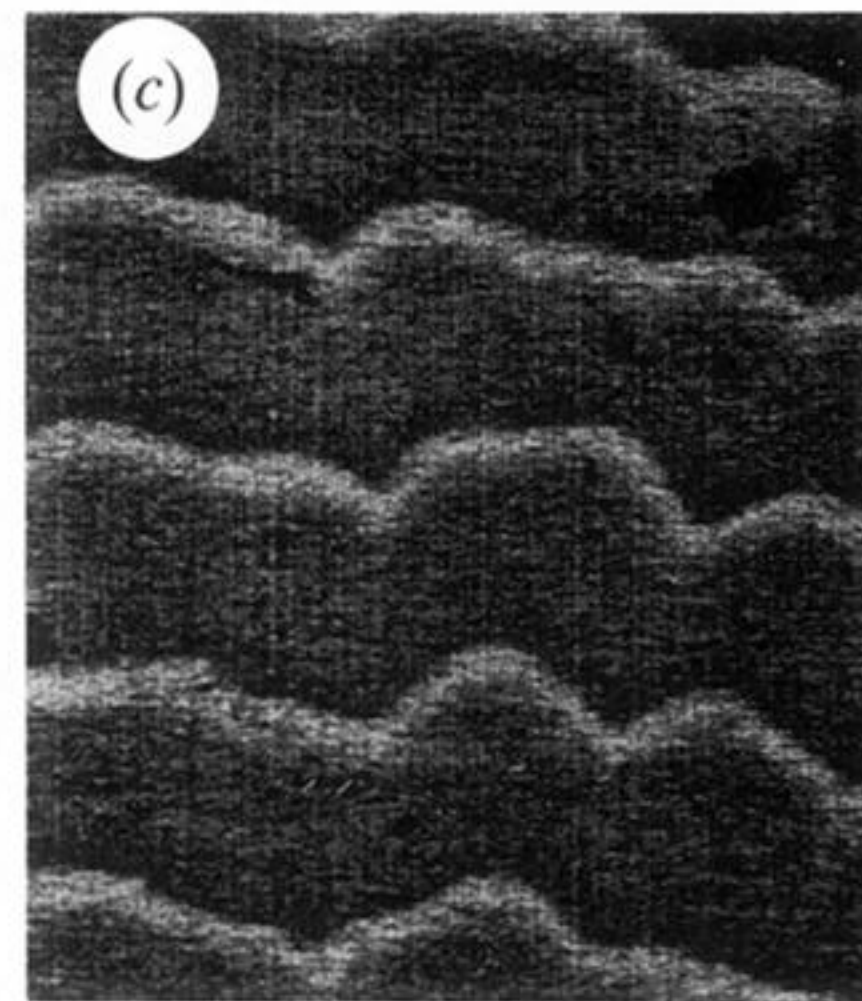
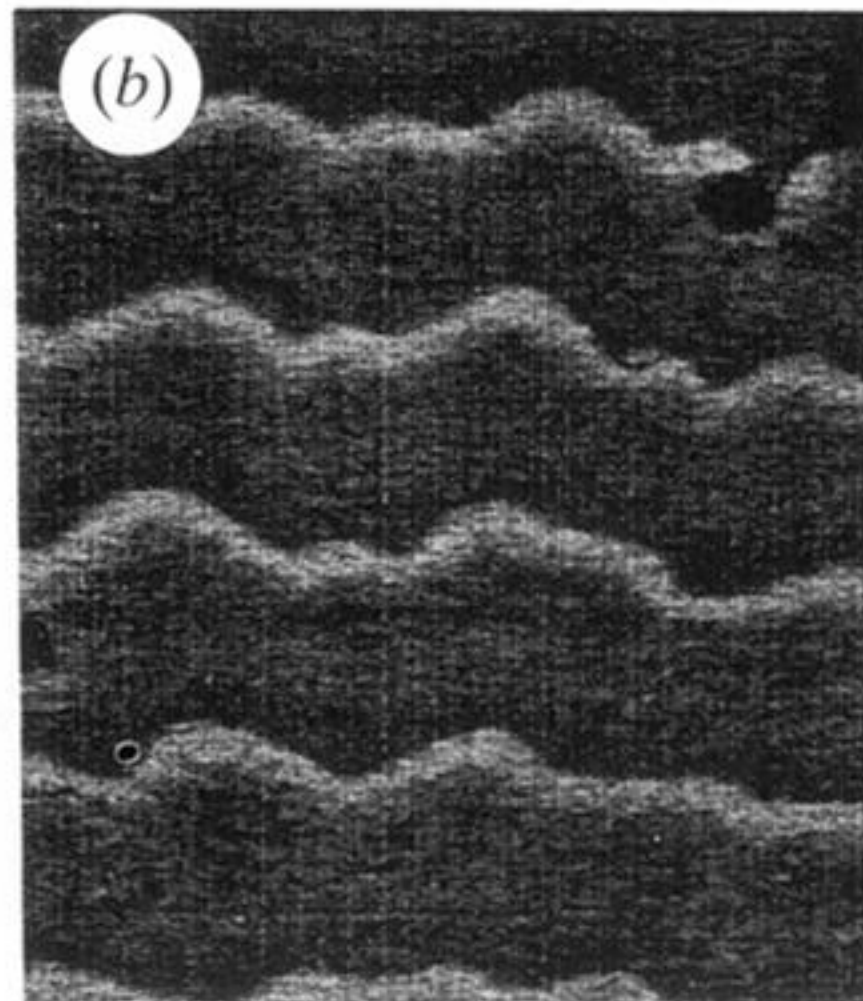
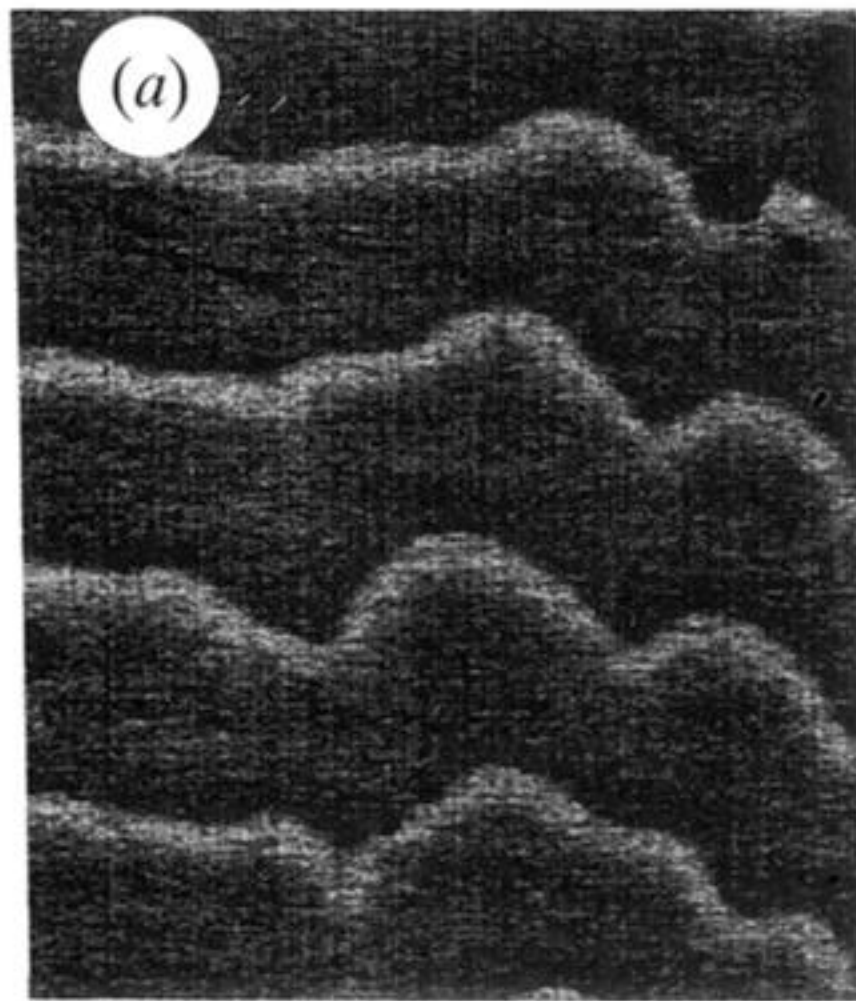


Figure 4. Wavefront instabilities ('ripples') in the same zone of the dish but at different times: (a) 0 min; (b) 3 min; (c) 6 min (30 000 lx, Ru-concentration: 1.0 mM).



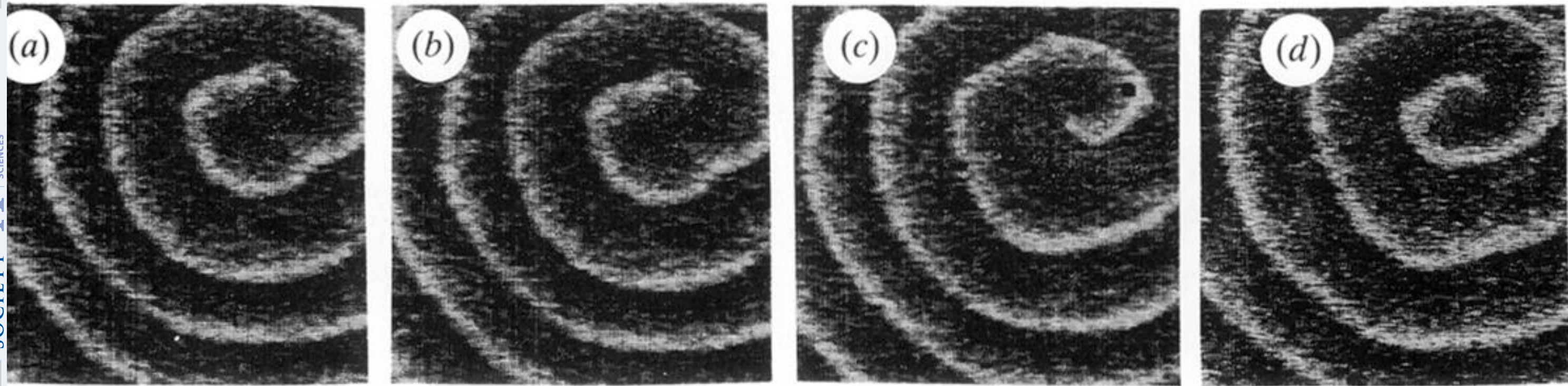
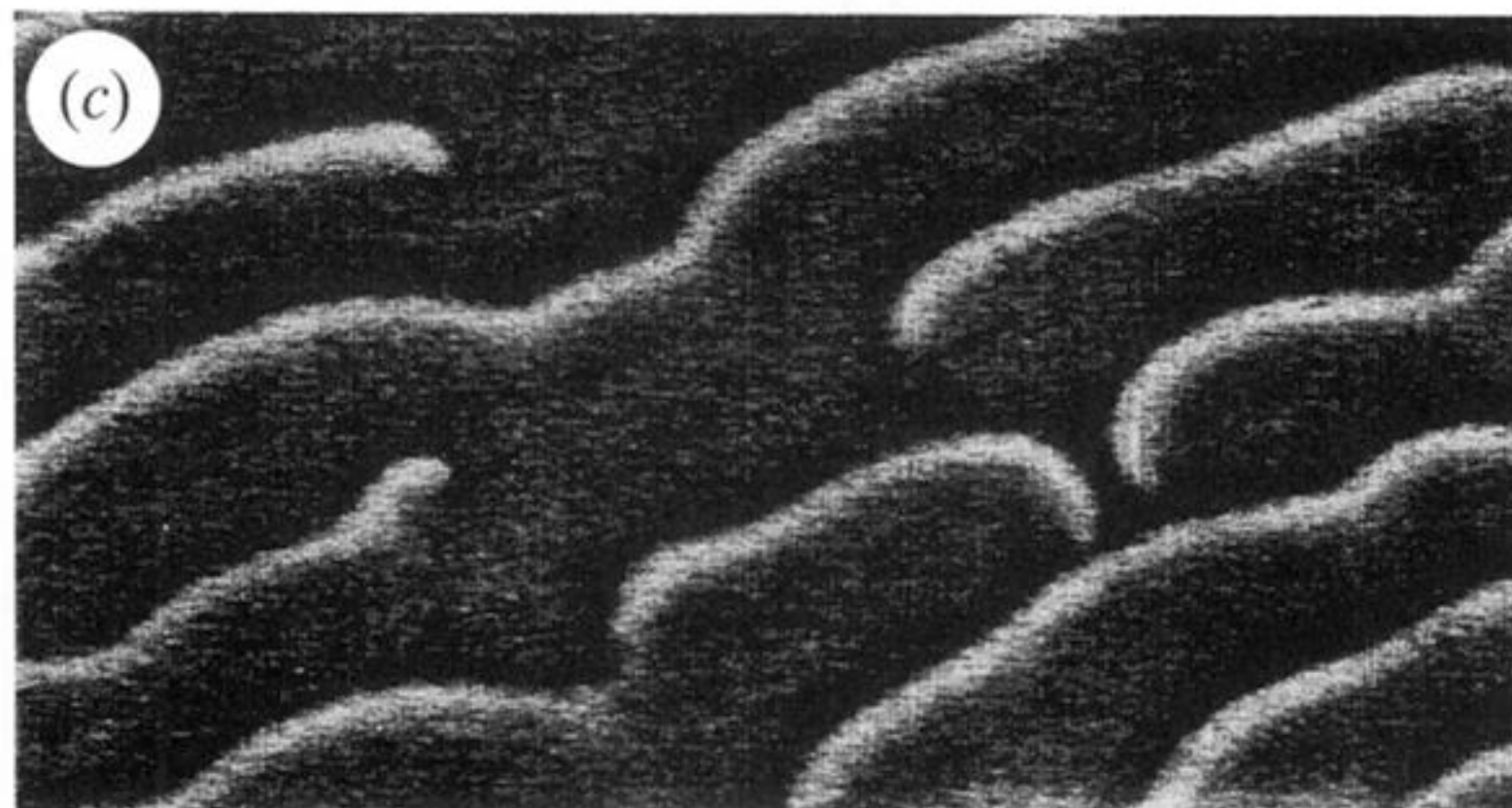
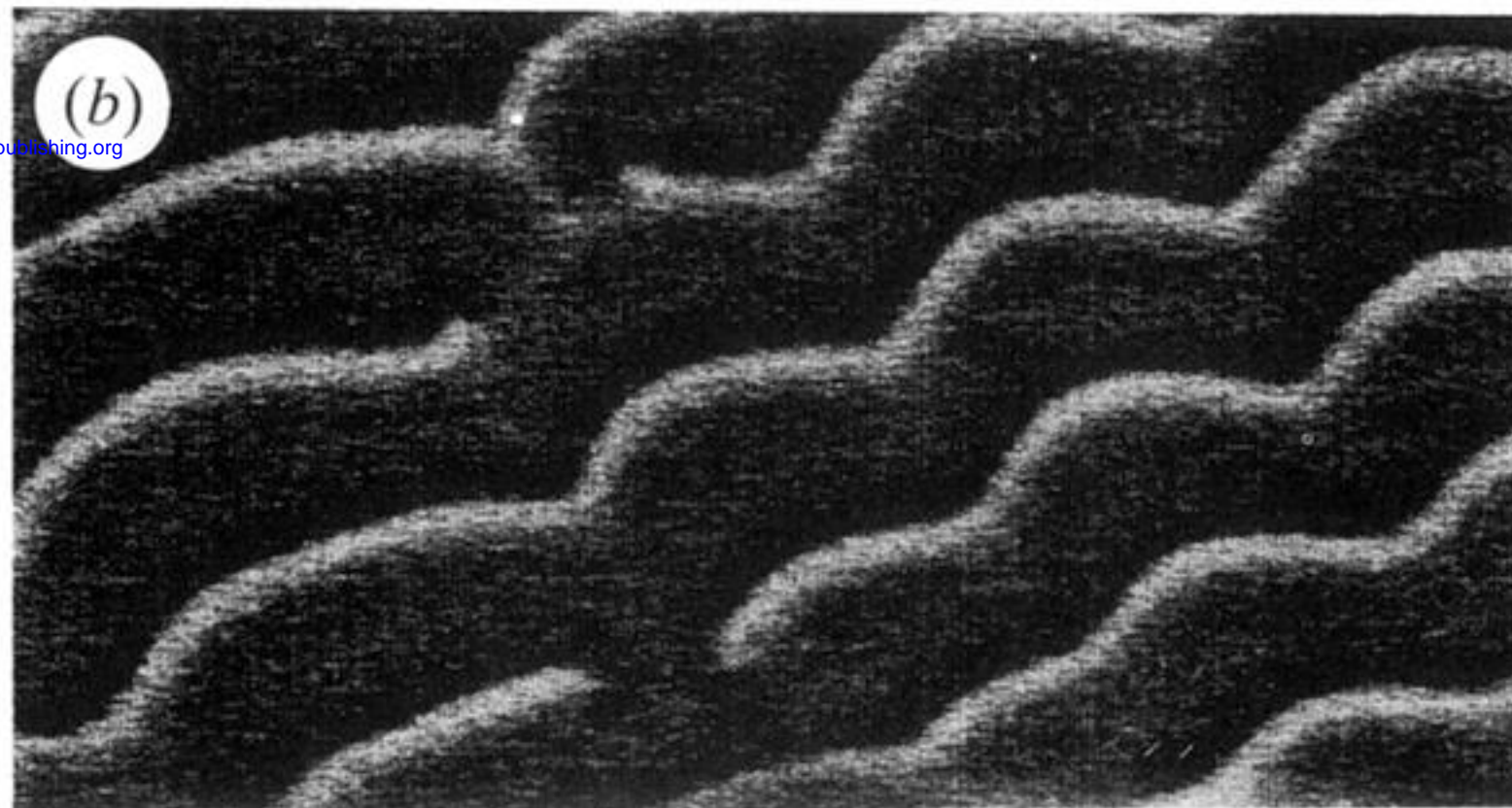
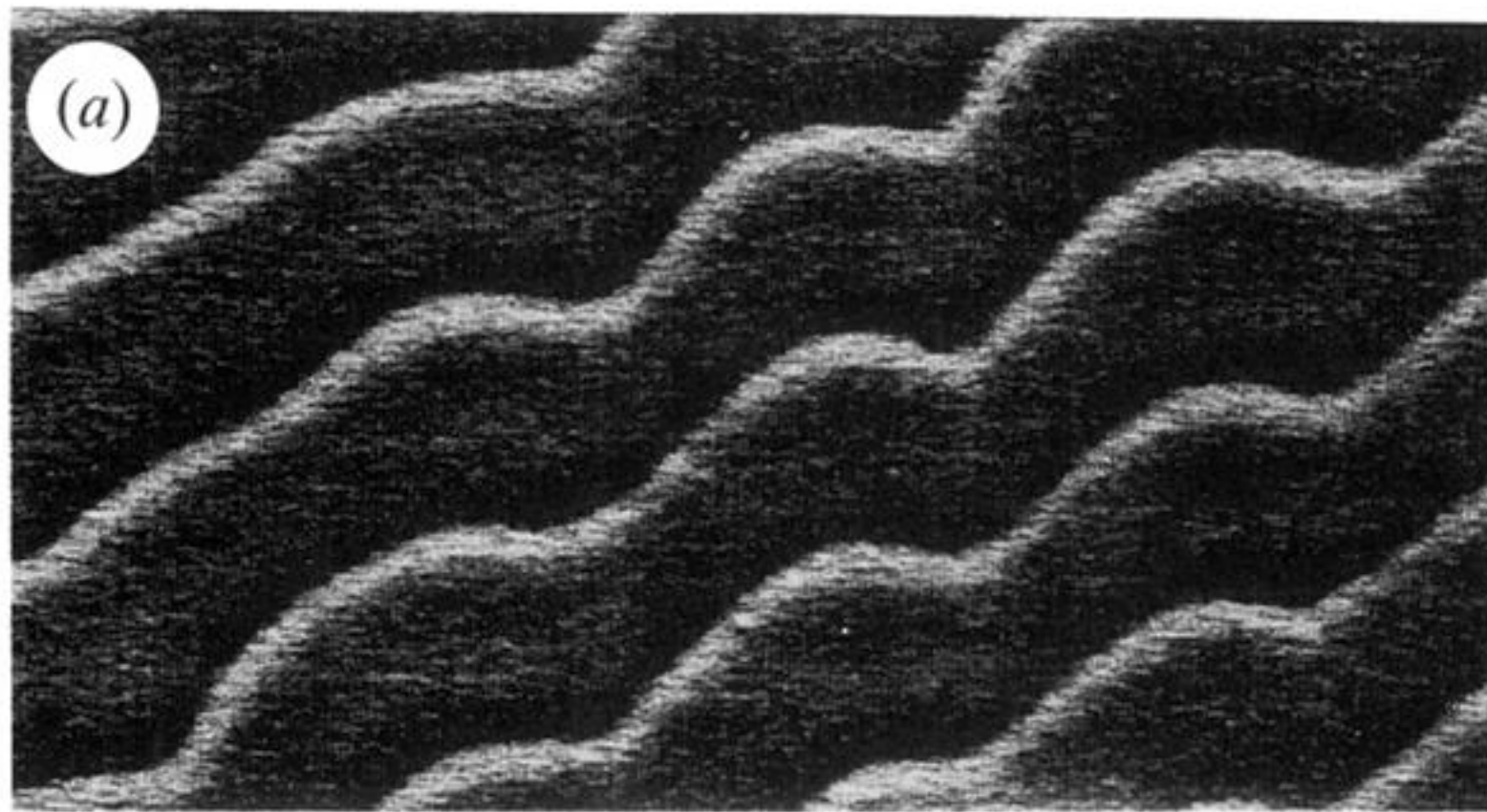


Figure 5. Unstable spiral at the following times: (a) 0 min; (b) 0.68 min; (c) 0.91 min; (d) 1.67 min (10 000 lx, Ru-concentration: 0.71 mM).





Downloaded from [rsta.royalsocietypublishing.org](https://rsta.royalsocietypublishing.org)

Figure 6. Breakdown of ripples ((a), time 0) into turbulent wave pieces at the following times: (b) 6.88 min; (c) 11.27 min (17 000 lx, Ru-concentration: 0.71 mM).